Advanced Vibration Analysis to Support Prognosis of Rotating Machinery Components

Michael J. Roemer
Gregory J. Kacpryznski
Rolf F. Orsagh
Impact Technologies
200 Canal View Blvd.
Rochester, NY 14623

Abstract
Advanced vibration analysis technologies that provide incipient fault detection to enable longer time horizons for failure prediction of critical machine components (Prognostics) has the potential to significantly reduce maintenance costs and increase availability and safety. This paper summarizes a comprehensive approach to enhancing prognostic accuracy through more intelligent utilization of relevant vibration diagnostic information coupled with advanced physics-of-failure modeling. Failures and associated predictions of critical rotating machinery components are used as a case study to introduce the concept of adapting key failure mode variables at a local damage-site based on fused vibration features. The overall prognostic system architecture is focused on minimizing inherent modeling and measurement uncertainties by updating material/fatigue properties, spall propagation rates etc., via sensed system measurements that evolve as damage progresses. A specific case study related to aircraft engine rolling element bearing is presented.

Introduction
Prognosis is the ability to predict or forecast the future condition of a component and/or system of components, in terms of failure or degraded condition, so that it can satisfactorily perform its operational requirement. In this paper, we will specifically focus on prognosis technologies that can enable the early detection and prediction of critical rotating machine components such as bearings and gears.

A specific aircraft engine bearing prognostic application is described that utilizes available measurement information, including rotor speed, vibration, lube system information and aircraft maneuvers to calculate remaining useful life for the engine bearings. Linking this sensed data with fatigue-based damage accumulation models associated with bearing remaining useful life is used to provide the predictive assessment. The combination of health monitoring data and model-based techniques provides a unique and knowledge rich capability that can be utilized throughout the components entire life, using model-based estimates when no diagnostic indicators are present and using the measured features at later stages when failure indications are detectable, thus reducing the uncertainty in model-based predictions.

Due to the inherent uncertainties in such prognosis systems, achieving the best possible prediction on a machine component's health is often implemented using various data fusion techniques that can optimally combine sensor data, empirical/physics-based models and historical information. Implementation of component-level, machinery prognostics will be illustrated on the engine bearing application.

Integrated Prognosis Framework

The approach described next provides an integrated prognosis framework as applied to rotating machinery components and it is generic in nature. In this case, it will be applied to rolling element bearings to fully describe the concept. The architecture builds upon existing or enabling technologies such as advanced oil debris/condition monitoring, high/low frequency vibration analysis, thermal trend analysis and empirical/physics-based modeling to practically achieve its objectives. An aspect of this approach is the development and implementation of an integrated prognostic architecture that is flexible enough to accept input from many different sources of diagnostic/prognostic information in order to contribute to better fault isolation and prediction on bearing remaining useful life.

The block diagram shown in Figure 1 illustrates this generic representation of the integrated prognosis system architecture for machinery component. Within this architecture, measured parameters from the health monitoring system such as oil condition/debris monitor outputs and vibration signatures can be accommodated within the anomaly detection/diagnostic fusion center. Based on these outputs, specific triggering points within the prognostic module can be processed so that effective transition associated with various failure mode models (i.e. spall initiation model to a spall progression model) can be accomplished.

Also shown in Figure 1, various sources of diagnostic information are combined in the model-based and feature-based prognostic integration algorithms for the specific bearing under investigation utilizing a probabilistic update process. Knowledge on how the specific bearing is being loaded, historical failure mode information and inspection data feedback can also be accommodated within this generic prognostic architecture. Finally, based on the overall component health assessment and prognosis, specific information related to remaining useful life and associated risk will be passed to operations and maintenance systems as an important input to that decision-making processes (covered in the last section of this chapter).

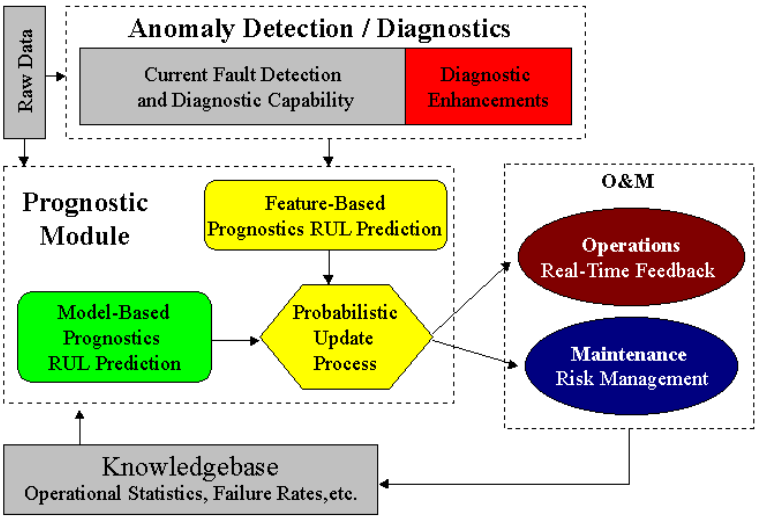

Figure 1-Integrated Diagnostic and Prognostic Capability

A more specific block diagram illustrating the implementation of this generic prognostic architecture as applied to a rolling element bearing is given in Figure 2. In this figure, features from oil analysis monitors are combined with vibration features in the "Anomaly and Diagnostics" module at the top. Once the appropriate feature extraction and fusion is performed, an output is passed to the "Physical Stochastic Model" that determines the current "state of

health" of the bearing in terms of failure mode progression. This health rating or status is utilized by the model to probabilistically weight the current "life-line location" in terms of the overall remaining useful life of the bearing. The fused features are also used as an independent measure of RUL that can be incorporated in the "update" process. The output of the module is a continuously updated description of the components current health state, as well as a projected RUL estimate based on its individual "signature" usage profile.

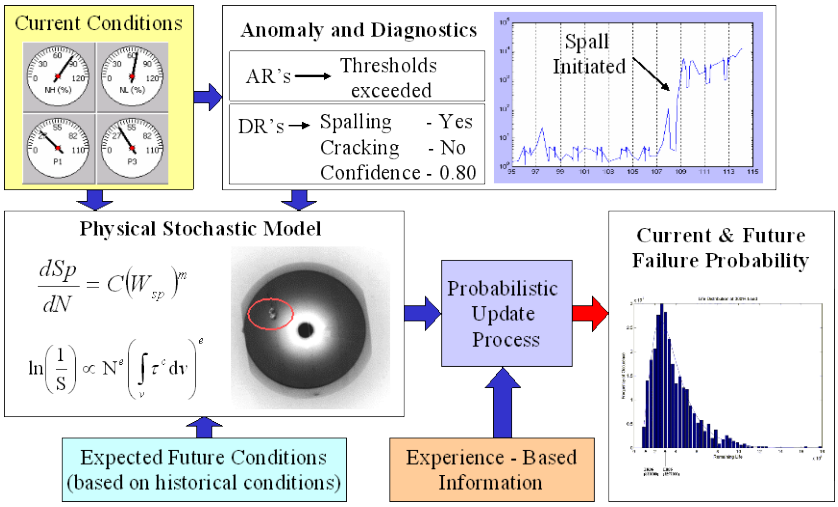

Figure 2- Bearing Prognostic and Health Management Module

Fusion for Bearing Prognosis

Data, information or knowledge fusion is the process of using collaborative or competitive information to arrive at a more confident decision both in terms of diagnostics and prognosis. Fusion plays a key role in advanced prognosis processes in terms of producing useful features, combining features, and incorporating model-based information. Within a comprehensive prognostic and health management system, fusion technologies are utilized in three main areas as shown in Figure 3. At the lowest level (Area 1), data fusion can be used to combine information from a multi-sensor data array to validate signals and create useful features. One example of this type of data fusion is combining a speed signal and a vibration signal to produce time synchronous average vibration features.

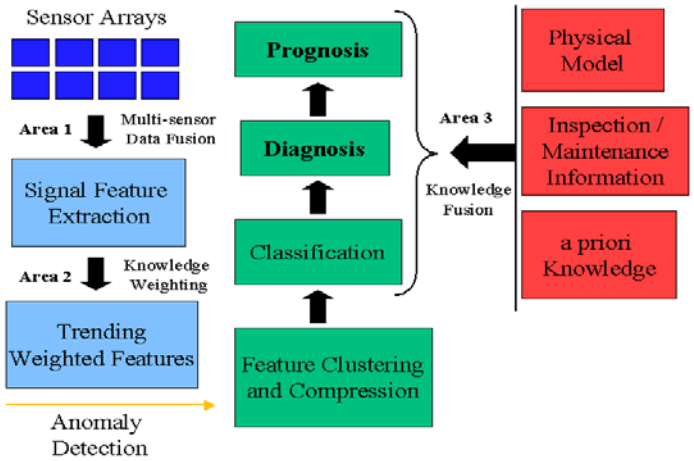

Figure 3-Health Management Fusion Application Areas

At a higher level (Area 2), fusion may be used to combine features in intelligent ways so as to obtain the best possible diagnostic information. This would be the case if a feature related to particle count and size in a bearing's lubrication oil was fused with a vibration feature such as RMS level. The combined result would yield an improved level of confidence about the bearing's health. Finally, Knowledge Fusion (Area 3) is used to incorporate experienced based information such as legacy failure rates or physical model predictions with signal-based information.

Identifying the optimal fusion architectures and approaches at each level is a vital factor in assuring that the realized system truly enhances the health monitoring and prognosis capabilities. Most current fusion implementations may be categorized as belonging to one of three generic architectures. These architectures are; Centralized, Autonomous, and Hybrid fusion, each with their own benefits with respect to a given application. Fusion of raw condition monitoring data or processed features can yield more robust diagnostic or prognostic information than individual condition indicators. Common fusion architectures such as the centralized fusion procedure combine multi-sensor data while it is still in its raw form. Another common approach, called autonomous fusion, addresses some of the data management problems encountered by the centralized architecture by placing feature extraction before the fusion process. In the case described herein, a hybrid fusion architecture as shown in Figure 4 takes the already processed features, classifies them on an individual basis and then fuses the result.

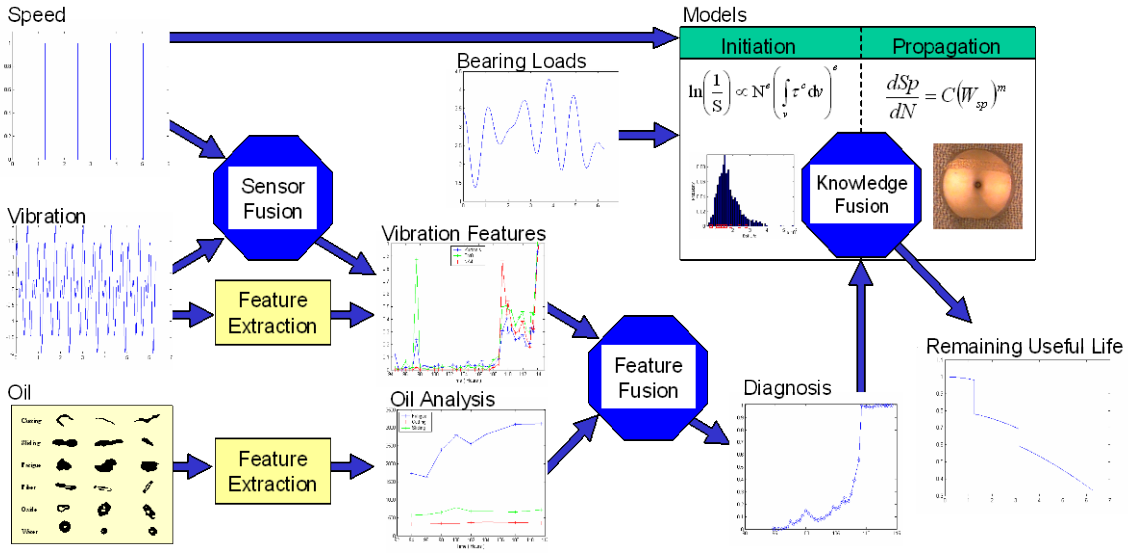

Figure 4 - Hybrid Fusion Architecture

As there are many different architectures for fusion, there are also many different algorithms themselves for performing the fusion. Simple information fusion techniques include weighted average and voting combinations of evidence from various sources. More sophisticated techniques, specifically Bayesian and Dempster-Shafer combination, are briefly described to illustrate the statistical basis and information requirements of these fusion techniques. Bayesian inference can be used to determine the probability that a diagnosis is correct, given a piece of a priori information. Analytically, Bayes' theorem is expressed as follows:

$$P(f_1|O_n) = \frac{P(O_n|f_1) \cdot P(f_1)}{\sum_{j=1}^{n} P(O_n|f_1) \cdot P(f_1)}$$

Where:

$P(f|O)$ = The probability of fault (f) given a diagnostic output (O), $P(O|f)$ = the probability that a diagnostic output (O) is associated with a fault (f), and $P(f)$ = the probability of the fault (f) occurring.

In the Dempster-Shafer approach, uncertainty in the conditional probability is considered. The Dempster-Shafer methodology hinges on the construction of a set, called the frame of discernment, which contains every possible hypothesis. Every hypothesis has a belief denoted by a mass probability (m). Beliefs are combined with the following equation.

$$Belief(Hn) = \frac{\sum_{A \cap B = Hn} m_i(A) \cdot m_j(B)}{1 - \sum_{A \cap B = 0} m_i(A) \cdot m_j(B)}$$

Early Fault Detection for Rolling Element Bearings

Development of specialized vibration or other features that can detect the incipient formation of a spall on a bearing race or rolling element is a critical step in the design of the integrated prognosis system mentioned above. To this end, a series of tests were designed and conducted to provide data for algorithm development, testing and validation. Vibration and oil debris data was acquired from a ball bearing test rig shown in Figure 5. A damaged bearing was installed and used to compare the effectiveness of various diagnostic features extracted from the measured data. The bearings are identical to the number 2 main shaft bearing of an Allison T63 gas turbine engine.

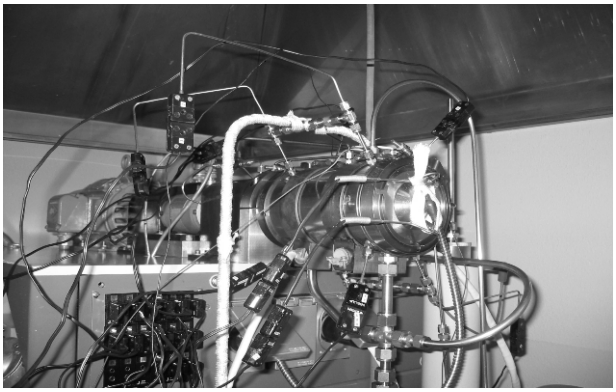

Figure 5 – Bearing Test Rig Setup

Although originally designed for lubrication testing, the Test Rig was used to generate accelerated bearing failures due to spalling. To accelerate this type of bearing failure, a fault was seeded into the inner raceway of one of the bearings by means of a small hardness indentation (Brinnell mark). The bearing was then loaded to approximately 14,234 N (3200 lbf) and ran at a constant speed of 12000 RPM (200 Hz). Vibration data was collected from a cyanoacrylate–mounted (common called Super Glue) accelerometer, which was sampled at over 200 kHz. Also,

the quantity of debris in the oil draining from the test head was measured using a magnetic chip collector (manufactured by Eateon Tedeco). The oil data was used in determining the severity of the spall progression.

Table 1 - Test Rig Bearing Dimensions (mm)

Bearing	Ball Diameter (Bd)	Number of balls (z)	Pitch Diameter (Pd)	Contact Angle (β)
# 1	4.7625	8	42.0624	18.5˚
# 2	7.9375	13	42.0624	18.5˚

The fundamental pass frequencies of the components of a bearing can be easily calculated with standard equations. Extraction of the vibration amplitude at these frequencies from a fast Fourier Transform (FFT) often enables isolation of the fault to a specific bearing in an engine. High amplitude of vibration at any of these frequencies indicates a fault in the associated component. Table 2 shows the calculated bearing fault frequencies.

Table 2 – Test Rig Bearing Fault Frequencies (Hz)

Shaft Speed	BSF	BPFI	BPFO	Cage
200	512	1530	1065	82

Note the listings are defined by: BSF: Ball Spin Frequency; BPFI: Inner Raceway Frequency; BPFO: Outer Raceway Frequency; Cage: Cage Frequency

High Frequency Enveloping Analysis

Although bearing characteristic frequencies are easily calculated, they are not always easily detected by conventional frequency domain analysis techniques. Vibration amplitudes at these frequencies due to incipient faults (and sometimes more developed faults) are often indistinguishable from background noise or obscured by much higher amplitude vibration from other sources including engine rotors, blade passing, and gear mesh in a running engine. However, bearing faults produce impulsive forces that excite vibration at frequencies well above the background noise in an engine.

Impact Energy™ is an enveloping-based vibration feature extraction technique that consists of first band pass filtering of the raw vibration signal. Second, the band pass filtered signal is full waved rectified to extract the envelope. Third, the rectified signal is passed through a low pass filter to remove the high frequency carrier signal. Finally, the signal's DC content is removed.

The Impact Energy™ process was applied to the seeded fault test data collected using the Bearing Test Rig. To provide the clearest identification of the fault frequencies, several band pass and low pass filters were used of analyze various regions of the vibration spectrum. Using multiple filters allowed investigation of many possible resonance's of the bearing test rig and its components. A sample Impact Energy™ spectrum from early in the Rig test is shown in Figure 6. Note that this data was collected prior to spall initiation (based on oil debris data), and the feature response is due the indentation on the race.

For comparison, a conventional FFT (10 frequency domain averages) of vibration data was also calculated and is shown in Figure 7. In the conventional frequency domain plot (Figure 7) there is

no peak at the inner race ball pass frequency (1530 Hz). However, the Impact Energy™ plot (Figure 6) shows clearly defined peaks at this frequency and the second through forth harmonics of the inner race ball pass frequency. These peaks were defined using a detection window of ± 5 Hz about the theoretical frequency of interest to account for bearing slippage. From the onset of the test there is an indication of a fault.

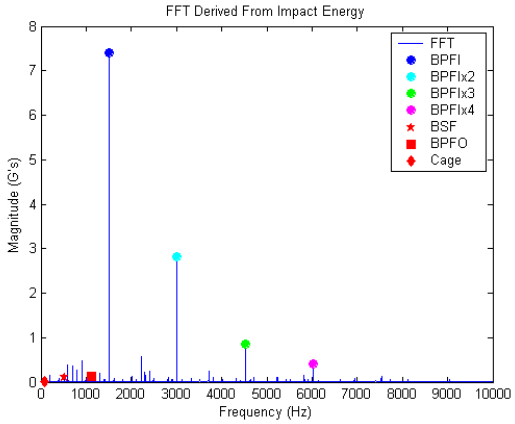

Figure 6 - Impact Energy™ FFT of Test Rig Bearing - Seeded Fault

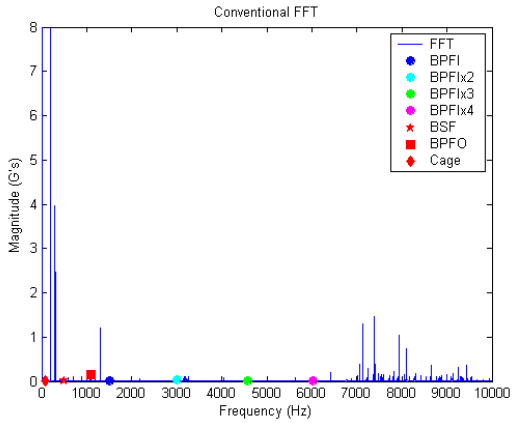

Figure 7 - Conventional FFT of Test Rig Bearing - Seeded Fault

Model-Based Analysis for Prognosis

A physics-based model is a technically comprehensive modeling approach that has been traditionally used to understand component failure mode progression. Physics-based models provide a means to calculate the damage to critical components as a function of operating conditions and assess the cumulative effects in terms of component life usage. By integrating physical and stochastic modeling techniques, the model can be used to evaluate the distribution of remaining useful component life as a function of uncertainties in component strength/stress properties, loading or lubrication conditions for a particular fault. Statistical representations of historical operational profiles serve as the basis for calculating future damage accumulation. The results from such a model can then be used for real-time failure prognostic predictions with specified confidence bounds. A block diagram of this prognostic modeling approach is given in Figure 8. As illustrated at the core of this figure, the physics-based model utilizes the critical life-dependent uncertainties so that current health assessment and future RUL projections can be examined with respect to a risk level.

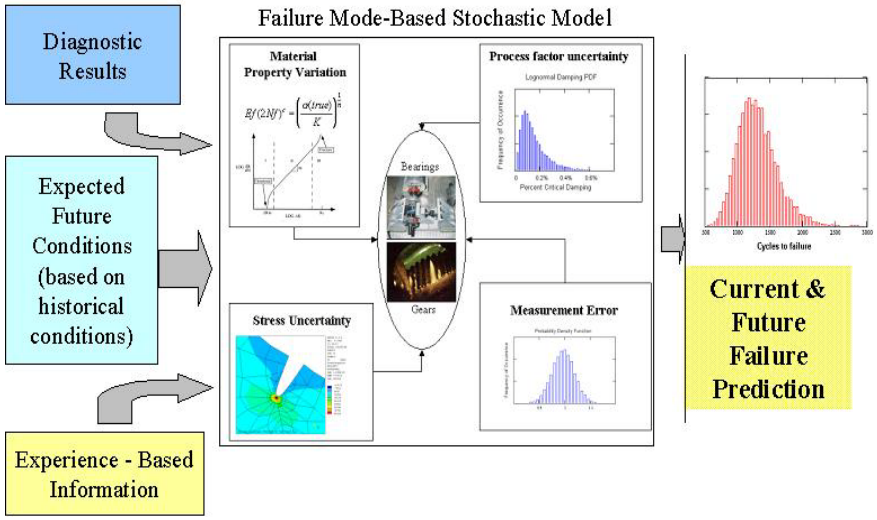

Figure 8 - Prognostic Bearing Model Approach

Model-based approaches to prognostics differ from feature-based approaches in that they can make RUL estimates in the absence of any measurable events, but when related diagnostic information is present (such as the feature described previously) the model can often be calibrated based on this new information. Therefore, a combination or fusion of the feature-based and model-based approaches provides full prognostic ability over the entire life of the component, thus providing valuable information for planning which components to inspect during specific overhauls periods. While failure modes may be unique from component to component, this combined model-based and feature-based methodology can remain consistent across different types of oil-wetted components in the rotating.

Bearing Spall Initiation and Propagation Models

Rolling-element contact fatigue is considered the primary cause of failure in bearings that are properly loaded, well aligned, and receive an adequate supply of uncontaminated lubricant. Rolling contact fatigue causes material to flake off from the load bearing surfaces of rolling elements and raceways leaving a pit or spall as shown in Figure 9.

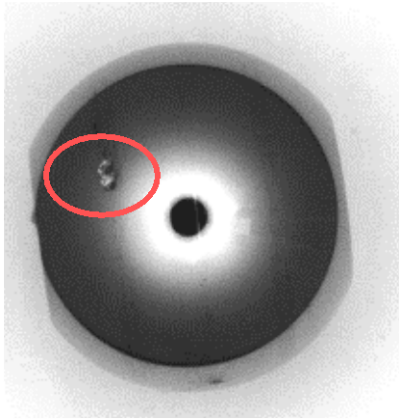

Figure 9 - Ball Bearing with Spall

Spalling of well-lubricated bearings typically begins as a crack below the load-carrying surface that propagates to the surface. Once initiated, a spall usually grows relatively quickly producing high vibration levels, and debris in the oil. Due to the relatively short remaining life following spall initiation, the appearance of a spall typically serves as the criteria for failure of bearings in critical applications.

Spall Initiation Model

A variety of theories exist for predicting spall initiation from bearing dimensions, loads, lubricant quality, and a few empirical constants. Many modern theories are based on the Lundberg-Palmgren (L-P) model [1] that was developed in the 1940's. A model proposed by Ioannides and Harris (I-H) [2] improved on the L-P model by accounting for the evidence of fatigue limits for bearings. Yu and Harris (Y-H) [3] proposed a stress-based theory in which relatively simple equations are used to determine the fatigue life purely from the induced stress. This approach depends to lesser extent on empirical constants, and the remaining constants may be obtained from elemental testing rather than complete bearing testing as required by L-P.

The fundamental equation of the Y-H model stated in equation 3 relates the survival rate (S) of the bearing to a stress weighted volume integral as shown below. The model utilizes a new material property for the stress exponent (c) to represent the material fatigue strength, and the conventional Weibull slope parameter to account for dispersion in the number of cycles (N). The fatigue initiating stress (τ) may be expressed using Sines multi-axial fatigue criterion [4] for combined alternating and mean stresses, or as a simple Hertz stress.

$$\ln\left(\frac{1}{S}\right) \propto N^e \left(\int_v \tau^c dv\right)^e$$

For simple Hertz stress, a power law is used to express the stress-weighted volume. In the equation below, λ is the circumference of the contact surface, and a and b are the major and minor axes of the contact surface ellipse. The exponent values were determined by Yu and Harris for b/a $\approx$0.1 to be x=0.65, y=0.65, and z=10.61. Yu and Harris assume that these values are independent of the bearing material.

$$\int_A \tau^c dA \cdot \lambda \propto a^x b^y \tau^z \lambda$$

According to the Y-H model, the life (L_{10}) of a bearing is a function of the basic dynamic capacity (Q_c) and the applied load as stated below. Where, the basic dynamic capacity is also given. A lubrication effect factor may be introduced to account for variations in film thickness due to temperature, viscosity, and pressure.

$$L_{10} = \left(\frac{Q_c}{Q}\right)^{\frac{x+y+z}{3}}$$

$$Q_C = A_1 \Phi D^{\frac{(2z-x-y)}{(z+x+y)}}$$

$$\Phi = \left[\left(\frac{T}{T_1} \right)^z \frac{u\left(D\Sigma\rho\right)^{\frac{(2z-x-y)}{3}}}{\left(a^*\right)^{z-x}\left(b^*\right)^{z-y}} \frac{d}{D} \right]^{\frac{-3}{z+x+y}}$$

Where:

A_1 = Material property
T = A function of the contact surface dimensions
T_1= value of T when a/b = 1
u = number of stress cycles per revolution
D = Ball diameter
ρ = Curvature (inverse radii of component)
d = Component (race way) diameter
a*= Function of contact ellipse dimensions
b*= Function of contact ellipse dimensions

A stochastic bearing fatigue model based on Y-H theory has been developed to predict the probability of spall initiation in a ball/V-ring test. The stochastic model accounts for uncertainty in loading, misalignment, lubrication, and manufacturing that are not included in the Y-H model. Uncertainties in these quantities are represented using normal and log normal probability distributions to describe the input parameters to the model. As a result, the stochastic Y-H model produces a probability distribution representing the likelihood of various lives.

Spall Progression Model

Once initiated, a spall usually grows relatively quickly producing increased amounts of oil debris, high vibration levels, and elevated temperatures that eventually lead to bearing failure. While spall progression typically occurs more quickly than spall initiation, a study by Kotzalas and Harris showed that 3 to 20 % of a particular bearings useful life remains after spall initiation. The study identified two spall progression regions. Stable spall progression is characterized by gradual spall growth and exhibits low broadband vibration amplitudes. The onset of unstable spall progression coincides with increasing broadband vibration amplitudes.

Kotzalas and Harris also presented a spall progression model. The model relates the spall progression rate (dS_p/dN) to the spall similitude (W_{sp}) using two constants (C and m) as shown below. The spall similitude is defined in terms of the maximum stress (σ_{max}), average shearing stress (τ_{avg}), and the spall length (S_p).

$$\frac{dSp}{dN} = C\left(W_{sp}\right)^m$$

$$W_{sp} = \left(\sigma_{\max} + \tau_{avg}\right)\sqrt{\pi Sp}$$

Spall progression data was collected during the Kotzalas/Harris study using a ball/V-ring test device. The data was collected at the Pennsylvania State University. Each of the lines shown in Figure 10 represents spall progression of a ball bearing. For one ball, indicated by multiple markers, the test was periodically suspended to measure the spall length. Only two spall length measurements, initial and final values, were taken for the other balls. The figure shows a large dispersion of the spall initiation life, which is indicated by the lowest point on each line. The

figure also shows a large dispersion of the spall progression life, which can be inferred from the slope of the lines.

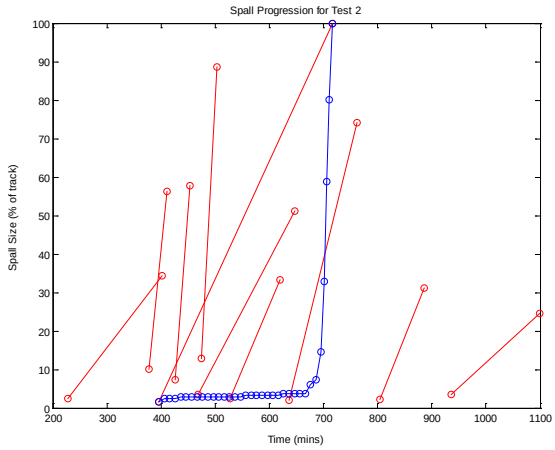

Figure 10 - Spall Progression Data from Phase I Analysis

The progression model was also applied to the Bearing Test Rig data acquired. A correlation between the recorded oil particle quantity and the spall size was determined from the initial and final quantities and spall sizes. This allowed scaling of the oil particle quantity to approximate spall size. The model agreed well with the spall progression during the test, as seen in Figure 11.

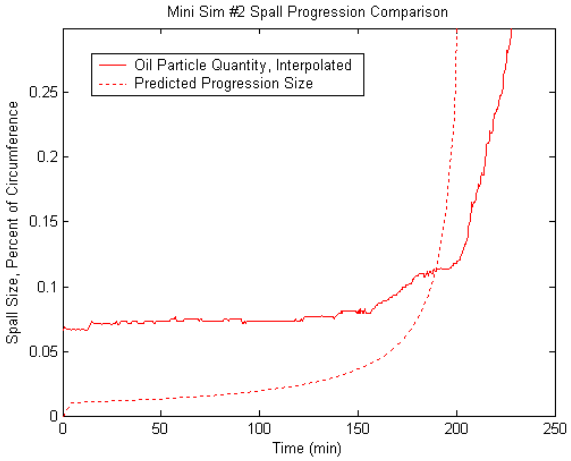

Figure 11 – Bearing Test Rig Spall Progression

A stochastic spall progression model based on Kotzalas/Harris theory was developed to predict the probability of spall progression in the ball/V-ring test. The stochastic model accounts for uncertainty in loading, misalignment, lubrication, and manufacturing that are not included in the Kotzalas/Harris model. As a result, the stochastic Kotzalas/Harris model produces a probability distribution representing the likelihood of various lives.

Prognosis Model Validation

Validation of the spall initiation model requires a comparison of actual fatigue life values to predicted model values. Acquiring sufficient numbers of actual values is not a trivial task. Under

normal conditions it is not uncommon for a bearing life value to extend past 100 million cycles, prohibiting normal run-to-failure testing.

Accelerated life testing is one method used to rapidly generate many bearing failures. By subjecting a bearing to high speed, load, and/or temperature, rapid failure can be induced. There are many test apparatus used for accelerated life testing including ball and rod type test rigs. One such test rig is operated by UES, Inc at the Air Force Research Laboratory (AFRL) at Wright Patterson Air Force Base in Dayton, OH. A simple schematic of the device is shown in Figure 12 with dimensions given in millimeters. This rig consists of three 12.7 mm diameter balls contacting a 9.5 mm rotating central rod see Table 2 for dimensions. The three radially loaded balls are pressed against the central rotating rod by two tapered bearing races that are thrust loaded by three compressive springs. A photo of the test rig is shown in Figure 13. Notice the accelerometers mounted on the top of the unit. The larger accelerometer is used to automatically shutdown the test when a threshold vibration level is reached, the other measures vibration data for analysis.

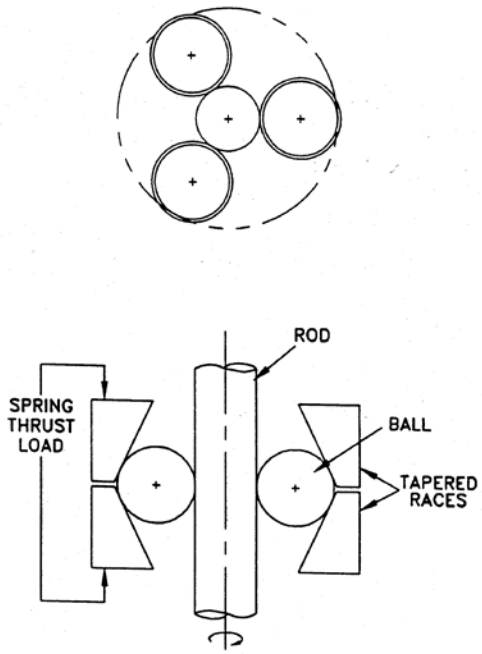

Figure 12 - Schematic of Rolling Contact Fatigue Tester

Table 2- Rolling Contact Fatigue Tester Dimensions (mm)

Rod diameter (Dr)	9.52
Ball diameter (Db)	12.70
Pitch diameter (Dm)	22.23

Figure 13 - Rolling Contact Fatigue Tester

By design the rod is subjected to high contact stresses. Due to the geometry of the test device, the 222 N (50 lbs) load applied by the springs translates to a 942 N (211 lbs) load per ball on the center rod. Assuming Hertzian contact for balls and rod made of M50 bearing steel, the 942 N radial load results in a maximum stress of approximately 4.8 GPa (696 ksi). This extremely high stress causes rapid fatigue of the bearing components and can initiate a spall in less than 100 hours, depending on test conditions including lubrication, temperature, etc. Since failures occur relatively quickly, it is possible to generate statistically significant numbers of events in a timely manner.

For validation purposes M50 rods and balls were tested at room temperature (23°C). The results of these tests are shown in Figure 14.

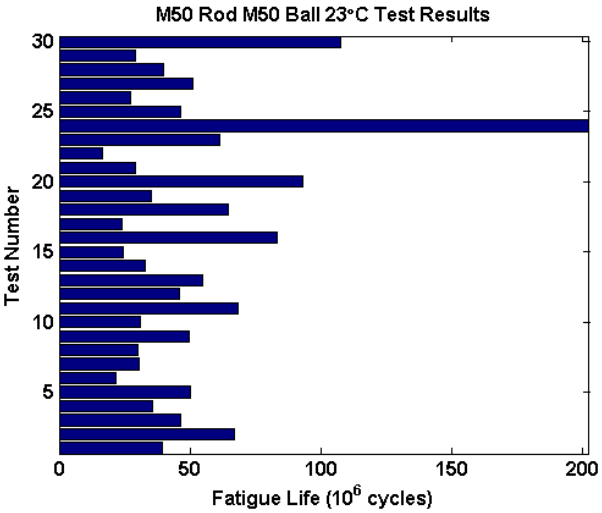

Figure 14 - RCF Fatigue Life Results

As stated above one of the issues with empirical/physics based models is their inherent uncertainty. Assumptions and simplifications are made in all modeling and not all of the model

variables are exactly known. Often stochastic techniques are used to account for the implicit uncertainty in a model's results. Statistical methods are used to generate numerous possible values for each input.

A Monte Carlo simulation was utilized in the calculation of the bearing life distribution. Inputs to the model were represented by normal or lognormal distributions to approximate the uncertainty of the input values. Sample input distributions to the model are shown in Figure 15.

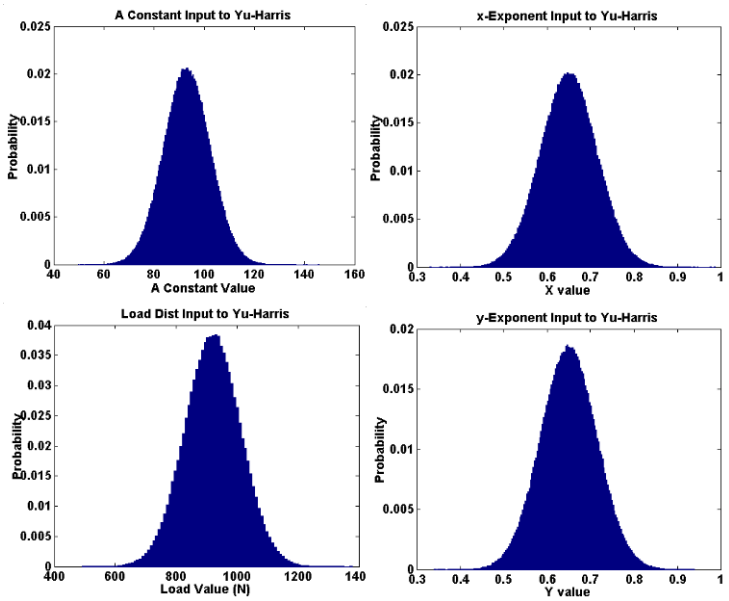

Figure 15 – Stochastic Model Input Distributions

The Yu-Harris model was used to simulate the room temperature M50 RCF tests. Figure 16 shows the results for a series of the room temperature RCF tests on the M50 bearing material. This test was run at 3600 RPM at room temperature with the 7808K lubricant. The y-axis is the number of central rod failures and the x-axis is the millions of cycles to failure. The predicted life from the model is also shown in Figure 16, superimposed on the actual test results. This predicted distribution shown in red was calculated from the model using one million Monte Carlo points.

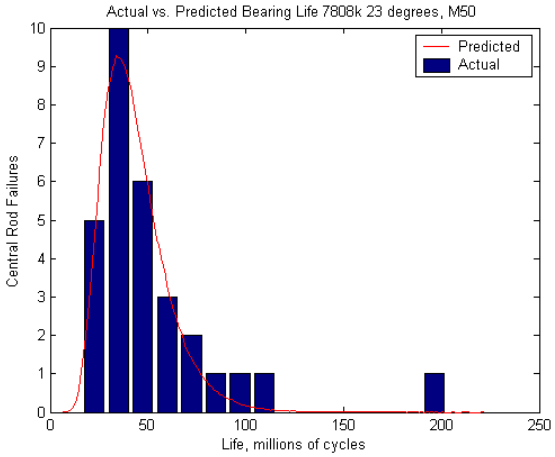

Figure 16 - Room Temp Results vs. Predicted

In Figure 17, the median ranks of the actual lives (blue dots) are plotted against the cumulative distribution function (CDF) of the predicted lives (blue line). The model predicted lives are slightly more conservative (in the sense that the predicted life is shorter than the observed life) once the cumulative probability of failure exceeds 70%. However since bearings are a critical component, the main interest is in the left most region of the distribution where the first failures occur and the model correlates better.

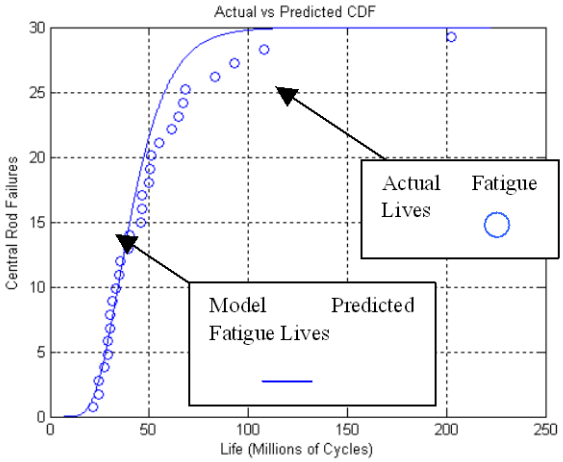

Figure 17 - Actual Life vs. Predicted Life

Calculation of median ranks is a standard statistical procedure for plotting failure data. During run-to-failure testing there are often tests that either are prematurely stopped before failure or a failure occurs of a component other than the test specimen. Although the data generated during these failures are the mode of interest, they provide a lower bound on the fatigue lives due to the failure mode of interest. One method for including this data is by median ranking.

The median rank was determined using Benard's Median Ranking method, which is stated in equation 6 below. This method accounts for tests that did not end in the failure mode of interest (suspensions). In the case of the ball and rod RCF test rig, the failure mode of interest is creation of a spall on the inner rod. The time to suspension provides a lower bound for the life of the test article (under the failure mode of interest), which can be used in reliability calculations. During the testing on the RCF test rig, significant portions of the tests were terminated without failure after reaching ten times the L_{10} life. There were also several tests that ended due to development of a spall on one of the balls rather than on the central rod.

$$\text{Benard's Median Rank} = \frac{(\text{AR} - 0.3)}{(\text{N} + 0.4)}$$

Where:

$\text{AR} = \text{Adjusted Rank}$

$\text{N} = \text{Number of Suspensions and Failures}$

The adjusted rank is calculated below.

$$\text{AR} = \frac{(\text{Reverse Rank})x(\text{Previous Adjusted Rank}) + (\text{N} + 1)}{\text{Reverse Rank} + 1}$$

Although the test does not simulate an actual bearing assembly in an engine, it does simulate similar conditions. Materials and the geometry of the bearing and the lubricants are the same for the test rig as they are in the T-63 engine. The test rig results validate the model's ability to predict the fatigue life of the material under similar conditions to an operating engine.

Conclusions

To achieve a comprehensive prognostic capability throughout the life of a rolling element bearing, model-based information can be used to predict the initiation of a fault before any diagnostic indicators are present. In most cases, these predictions will prompt "just in time" maintenance actions to prevent the fault from developing. However, due modeling uncertainties, incipient faults may occasionally develop earlier than predicted. In these situations, sensor-based diagnostics complement the model-based prediction by updating the model to reflect the fact that fault initiation has occurred. Sensor-based approaches provide direct measures of component condition that can be used to update the modeling assumptions and reduce the uncertainty in the RUL predictions. Subsequent predictions of the remaining useful component life will be based on fault progression rather than initiation models.

References

1. Ioannides, and Harris, "A New Fatigue Life Model for Rolling Bearings", Journal of Tribology, Vol. 107, pp. 367-378, 1985

2. Yu, and Harris, "A New Stress-Based Fatigue Life Model for Ball Bearings", Tribology Transactions, Vol. 44, pp. 11-18, 2001

3. Sines, and Ohgi, "Fatigue Criteria Under Combined Stresses or Strains", ASME Journal of Eng. Materials and Tech., Vol. 103, pp. 82-90, 1981

4. Toth, Douglas K., Saba, Costandy S., Klenke, Christopher J. "Minisimulator for Evaluating High-Temperature Canidate Lubricants Part I- Method Development," University Dayton Research Institute-Aero Propulsion Directorate USAF, Dayton, OH, 2001.

5. Glover, Douglas. "A Ball-Rod Rolling Contact Fatigue Tester," *Rolling Contact Fatigue Testing of Bearing Steels, ASTM STP 771*, ASTM, 1982, pp. 107-125.

6. Harris, T. (4th Edition 2001), *Rolling Bearing Analysis*, John Wiley & Sons, New York.

7. Wensig, J. A.," On the Dynamics of Ball Bearings," PhD Thesis, University of Twente, The Netherlands, pp 90, 1998.

8. Hartman, W., and Hess, A., "A USN Strategy for Mechanical and Propulsion System Prognostics with Demonstration Results" AHS Forum 58, Quebec, Canada, June 11-13, 2002.

9. Kacprzynski, G., et al., "Calibration of Failure Mechanism-Based Prognosis with Vibratory State Awareness Applied to the H-60 Gearbox" Proceedings of the 2003 IEEE Aerospace Conf., Big Sky, MT.

10. Roemer, M., and Kacprzynski, G., "Development of Diagnostic and Prognostic Technologies for Aerospace Health Management Applications" 2001 IEEE Aerospace Conf., Big Sky, MT.